ELSEVIER

Food Hydrocolloids 15 (2001) 107–115

FOOD HYDROCOLLOIDS

www.elsevier.com/locate/foodhyd

Aggregation in a concentrated model protein system: a mesoscopic simulation of β-casein self-assembly

Eric Dickinson*, Sujata Krishna

Procter Department of Food Science, University of Leeds, Leeds LS2 9JT, UK

Received 28 July 2000; revised 9 October 2000; accepted 2 November 2000

Abstract

A mesoscopic model of a concentrated system of amphiphilic co-polymer molecules has been investigated in three dimensions by Brownian dynamics computer simulation. Each co-polymer species consists of a flexible bonded chain of four hydrophilic segments and 12 hydrophobic segments. Equilibrium configurations have been generated as a function of the polymer volume fraction and the strengths of the hydrophobic and electrostatic segment–segment interactions. Some quantitative data are reported on segment co-ordination numbers, maximum aggregate sizes and diffusion coefficients. The mesoscopic simulation approach is put forward as a simple systematic way of modelling a solution of β-casein-like molecules under concentrated conditions. Subject to suitable modifications and refinements, this approach provides a framework for investigating effects of protein concentration and solution conditions on the structure of self-assembled casein systems in food gels and emulsions. © 2001 Elsevier Science Ltd. All rights reserved.

Keywords: β-Casein; Computer simulation; Protein aggregation; Self-assembly

1. Introduction

Brownian dynamics simulations of concentrated systems of aggregating spherical particles can give valuable insight into the relationship between interparticle interactions during and after gelation and the physical properties of the resulting particle gel networks (Bijsterbosch, Bos, Dickinson, van Opheusden, & Walstra, 1995; Dickinson, 1997; Whittle & Dickinson, 1997; Lodge & Heyes, 1999; Mellema, van Opheusden, & van Vliet, 1999). Casein micelles, the basic building blocks of acid-induced and rennet-induced milk gels, are roughly spherical and of colloidal size ($\sim 10^{-7}$ m). Hence, Brownian dynamics simulation of systems of spherical particles has been useful for describing rheology and structure of casein gels formed from aggregated casein micelles. However, the use of simple spherical building blocks is clearly inappropriate for defining structure on the smaller spatial scale ($\sim 10^{-8}$ m) of the size of individual casein molecules or small clusters. On this more detailed scale, any proper interpretation of the structure must account for the chain-like character of the self-assembling polymeric amphiphiles (Horne, 1998).

The purpose of the present paper is to introduce a modelling approach to describe the self-assembly of concentrated casein solutions. The scope includes solutions of the individual pure caseins (α_{s1}-casein, β-casein, etc.), as well as casein mixtures (e.g. as in commercial sodium caseinate), and the effects of variables such as pH and salt concentrations. The spatial and temporal character is mesoscopic—beyond that of any individual molecular groups (e.g. amino-acid residues) but having some of internal molecule features of casein as a polymeric surfactant. The approach adopted is to represent the disordered protein as a linear oligomeric co-polymer of spherical segments of more than one type (Ganazzoli, 2000). Though our initial designation here involves just two segment types, hydrophilic and hydrophobic, the model can be readily generalized to generate more advanced representations.

The most extensively studied of the casein monomers is bovine β-casein. This protein has all the key characteristics of an excellent surface-active agent and polymeric stabilizer. It is a flexible linear polyelectrolyte of not too high molecular weight (209 amino-acid residues) carrying a moderate net charge (-15 e) at neutral pH. Its highly non-uniform distribution of hydrophilic and hydrophobic amino-acid residues produces a distinctly amphiphilic molecular structure that resembles a simple water-soluble surfactant or a block co-polymer. At moderately low concentrations β-casein self-assembles into roughly spherical

* Corresponding author. Tel.: +44-1132-332956; fax: +44-1132-332982.

E-mail address: e.dickinson@leeds.ac.uk (E. Dickinson).

0268-005X/01/$ - see front matter © 2001 Elsevier Science Ltd. All rights reserved.
PII: S0268-005X(00)00057-6

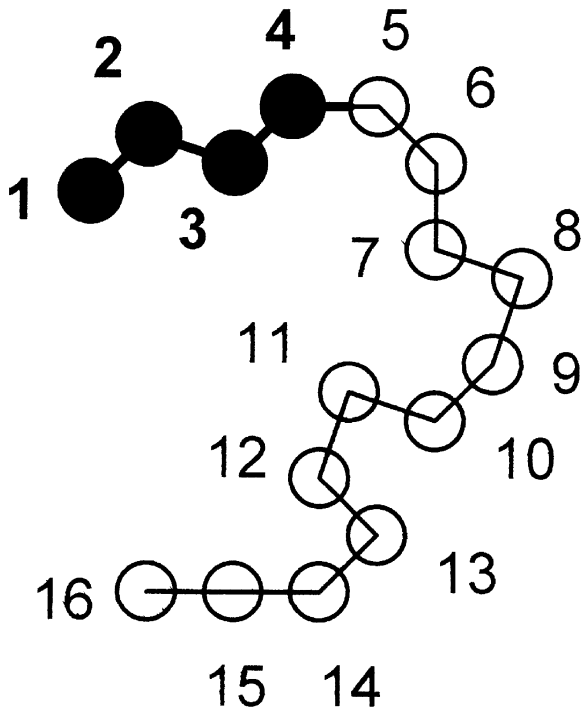


Fig. 1. Schematic representation of flexible amphiphilic block co-polymer consisting of four hydrophilic segments (●) and 12 hydrophobic segments (○).

surfactant-like micelles (Schmidt, 1982; Leclerc & Calmettes, 1997). This reversible self-association is mainly driven by attractive hydrophobic interactions, and the extent of aggregation increases with temperature and ionic strength (Schmidt & Payens, 1972). Based on a wide range of experimental evidence, it can be reliably inferred (Dalgleish, 1996; Dickinson, 1998, 1999) that β-casein adsorbs with its extensive hydrophobic region anchored directly at the surface and its hydrophilic region (40–50 segments at the N-terminus) protruding extensively into the aqueous phase. This representation has been given support by polymeric modelling of β-casein adsorption using self-consistent-field theory (Leermakers, Atkinson, Dickinson, & Horne, 1996). The calculations demonstrate the crucial role of the cluster of charged phosphoserine residues in β-casein in maintaining the steric stabilizing layer, whilst also preventing interfacial precipitation (multilayers). The phosphoserine-rich 'blob' can be considered to be repelled from the surface by electrostatic forces, but restrained from moving into the bulk solution by a stretched 'spring' section anchored strongly to the surface by the hydrophobic groups (Horne & Leaver, 1995). Like its adsorption behaviour, the reversible micellization of β-casein in aqueous solution is sensitive to the balance of hydrophobic and electrostatic interactions within the amphiphilic polymer molecule. Removal of just the last 20 residues at the hydrophobic *C*-terminus destroys the protein's ability for self-association in aqueous solution (Berry & Creamer, 1975).

Native casein, and the sodium caseinate derived from it, is a mixture of several different individual casein species (mainly α_{s1}, α_{s2}, β and κ). Like β-casein, κ-casein forms soap-like micelles in solution (Vreeman, Brinkhuis, & van der Spek, 1981). But α_{s1}-casein forms long worm-like aggregates through a series of consecutive association steps (Schmidt & Payens, 1972; Schmidt, 1982). In dilute solution, sodium caseinate has long been generally considered to exist as small spherical sub-micellar particles (10–20 nm) in equilibrium with free casein molecules (Creamer & Berry, 1975). More recently, dynamic light-scattering studies have suggested that the caseinate sub-micellar species may coexist with supramolecular assemblies (Chu, Zhou, Wu, & Farrell, 1995), osmotic pressure data have been interpreted in terms of rod-like aggregates at high concentrations (Farrer & Lips, 1999), and combined light scattering and size-exclusion chromatography has indicated (Lucey, Srinivasan, Singh, & Munro, 2000) a wide range of molecular weight species, including some highly non-spherical micelles and polymers of κ-casein. However, in the absence of definitive scattering data for concentrated systems (X-rays or neutrons), the influence of protein composition on the structure of highly interacting self-assembled casein solutions still remains largely unknown.

In this preliminary simulation study, we explore how the aggregation state of the model system of linear co-polymer oligomers is affected by the relative interaction strengths of the hydrophilic and hydrophobic segments. In constrast to some other studies in this field (Toma & Toma, 2000), we adopt a continuum (non-lattice) approach. The proportions of the two types of segments assigned to the co-polymer chain are meant to correspond roughly to that of β-casein. Nonetheless, the emphasis at this stage is on generic aspects, rather than on trying to fit the simulation results to any specific set of experimental data.

2. The model

We consider a di-block co-polymer consisting of 16 rigid spherical segments connected together into a flexible linear chain as illustrated in Fig. 1. This is a mesoscopic model in which each effective segment is meant to represent between 10 and 15 amino-acid residues along a linear polypeptide chain. As discussed in the recent dynamic lattice Monte Carlo simulation of Anderson, Pande, and Radke (2000), such effective segments are referred to in the polymer physics literature as Kuhn segments (Boyd & Phillips, 1993). Each segment has a hard-sphere diameter of 2 nm, and each flexible segment–segment bond has an equilibrium length of 0.5 nm. Segments 1–4 are hydrophilic in character and segments 5–16 are hydrophobic. This subdivision is meant to mirror the amphiphilic character of the β-casein molecule. The set of co-polymer segments 1–4 is meant to represent the sequence of 50 amino-acid residues at the N-terminus of the β-casein molecule; this tail region is known to be highly hydrophilic and to contain all

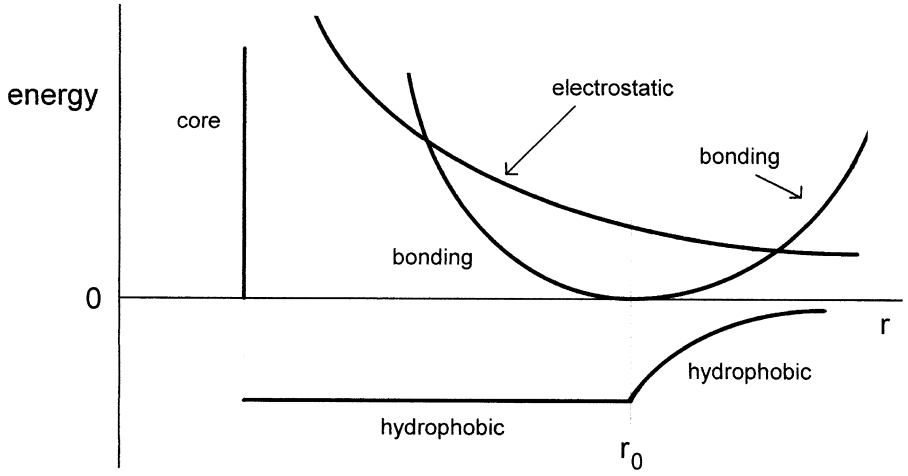


Fig. 2. Illustration of energy *versus* distance plot for the various contributions to segment–segment potential from core interaction, hydrophobic interaction, electrostatic interaction and bonding interaction. The distance r_0 corresponds to the equilibrium bond length.

five phosphoserine residues. Co-polymer segments 5–16 represent the rest of the β-casein molecule, which is substantially hydrophobic and carries no net charge.

Pairs of segments on the same or different chains interact at short-range with a hard-sphere repulsive potential

$$u_{hs} = \infty, \quad (r < \sigma) \qquad 0, \quad (r \geq \sigma) \tag{1}$$

where r is the centre-to-centre separation. Hydrophobic segments on the same chain (non-adjacent) or different chains interact with an attractive potential of the form:

$$u_h = \begin{cases} -\epsilon_h, & (r \leq r_0) \\ -\epsilon_h(r_0/r)^6, & (r_0 < r \leq r_c) \\ 0, & (r_c < r) \end{cases} \tag{2}$$

Table 1
Standard set of parameter values used in the simulations (with time step and interaction energies given in reduced units)

Parameter	Value
Segment diameter (σ)	2 nm
Segment volume fraction (ϕ)	0.2
Medium viscosity (η_s)	1.19 mPa s
Segment diffusion coefficient (infinite dilution)	1.85×10^{-6} cm^2 s^{-1}
Unit time	3.16×10^{-11} s
Time step (Δt)	0.1
Temperature (T)	300 K
Bond energy (ϵ_b)	1.0
Equilibrium bond length (r_0)	2.5 nm
Maximum bond length	4 nm
Hydrophobic interaction energy (ϵ_h)	0.05
Electrostatic interaction energy (ϵ_e)	1.0
Hydrophobic/electrostatic cut-off distance (r_c)	4 nm

where ϵ_h is the hydrophobic interaction energy parameter, r_0 is the bond length (= 2.5 nm), and r_c is the cut-off distance for the hydrophobic interaction (taken as 4 nm). Hydrophilic segments on the same chain (non-adjacent) or different chains interact with a repulsive screened electrostatic potential (Brooks, Bruccoleri, Olafson, States, Swaminathan, & Karplus, 1983),

$$u_e = \begin{cases} (q^2\epsilon_e/4\pi\epsilon_r r)[1 + (r/r_c)^4 - 2(r/r_c)^2], & (r<r_c) \\ 0, & (r_c \leq r) \end{cases} \tag{3}$$

where ϵ_e is the electrostatic interaction energy parameter, ϵ_r is the relative permittivity (taken as 80), q is the notional segment charge, and r_c is the electrostatic cut-off range parameter (taken as 4 nm).

Adjacent segments along the chain are held together permanently by a Morse bonding potential (Morse, 1929),

$$u_b = \epsilon_b\{\exp(\rho(r_0 - r)/r_0)[\exp(\rho(r_0 - r)/r_0) - 2]\}, \tag{4}$$

where ϵ_b is the bond energy, r_0 is the equilibrium bond length (2.5 nm), and ρ is a parameter related to the ease of stretching of the bond. Decreasing ρ increases the attractive range of the bonding potential and softens its repulsive wall. With $\rho = 6$, the Morse potential has the same curvature as the Lennard-Jones 12:6 potential near $u_b = -\epsilon_b$. Here we choose a relatively soft bonding interaction with $\rho = 4$ in order to allow a large simulation timestep. The maximum allowed bond length is set at 4 nm.

Fig. 2 shows a schematic diagram of the bonding potential and the three contributions to the non-bonding interaction (core, electrostatic and hydrophobic). The state of aggregation of the chains is mainly determined by the relative strengths of the electrostatic and hydrophobic interaction energies, ϵ_h and ϵ_e. The standard set of values of the simulation parameters are given in Table 1. Typically, we express distance, energy and time in terms of the reduced units of σ, k_BT and $\sigma(m/k_BT)^{1/2}$, where k_B is Boltzmann's

contant, T is the absolute temperature, and m is the particle mass. Unless otherwise stated the values adopted in the simulations are as Table 1.

As compared with a 'real' protein like β-casein, our model co-polymer is simplified both in terms of the number of segment types and the nature of the segment–segment interactions. So, the model has notional electrical charge density distributed evenly across four identical mesoscopic hydrophilic segments, whereas the important charged phosphoserines on the 'tail' region of β-casein are known to be clustered (residues 15–19, with an intervening leucine). Similarly, the 12 mesoscopic hydrophobic segments of our model co-polymer are all identical in nature and interactions, whereas in reality there are some polar and even charged amino-acid side-chains within the main 'non-tail' region of β-casein. As for our adopted functional forms for the non-bonded interactions in Eqs. (1)–(3), these were chosen to have approximately the correct absolute energies and relative ranges (see Fig. 2), and to be computationally convenient—without any particular desire on our part to attempt to describe quantitatively the specific types of interactions between the molecular centres. Hence, what we call 'hydrophobic' segments in our mesoscopic model are not meant to have interactions that exactly match the form of hydrophobic forces interferred, for instance, from atomic scale modelling. Equally, for the segments with electrostatic interactions, we do not explicitly consider charge screening in the functional form (Eq. (3)), although clearly a dependence on ionic strength could, in principle, be mapped onto variations in the parameter ϵ_e.

3. Simulation methodology

The properties of a system of 81 excluded-volume chains (*i.e.* $N = 81 \times 16 = 1296$ particles) were simulated in a cubic cell with periodic boundary conditions usng the numerical technique of Brownian dynamics (Allen & Tildesley, 1989). The polymer volume fraction was varied by adjusting the box size. A typical timestep of $\Delta t = 0.1$ (in reduced program units) was used. The maximum timestep is determined by the steepness of the bonding potential. The timestep needs to be the minimum to allow momentum relaxation to occur. This is a key condition for Brownian dynamics, since the approach assumes that the behaviour of the suspending fluid of viscosity η_s can be temporally averaged so that the system dynamics is described by the Langevin equation

$$m\dot{r} = \xi\dot{r} + F_i(t) + R_i(t), \tag{5}$$

where F_i is the net force on particle i, $\xi = 3\pi\eta_s\sigma$ is the Stokes friction coefficient, and R_i is the Langevin random force which must obey the conditions:

$$\langle R(t)\rangle = 0,\ \langle R(t)R(t)\rangle = 2k_BT\Delta t. \tag{6}$$

A finite difference integration of Eq. (5) is used to describe the evolution of particles through time and space. The translational update algorithm is

$$r_i(t+\Delta t) - r_i(t) = F_i(t)\xi^{-1}\Delta t + R_i(t,\Delta t), \tag{7}$$

where F_i is the force on particle i due to interparticle interactions and $R_i(t, \Delta t)$ is the familiar Gaussian random displacement.

A novel procedure was devised for efficiently setting up the initial random distribution of non-overlapping co-polymer chains. The starting point was a random distribution of spherical particles corresponding to an assembly of N unbonded segments. This arrangement was then allowed to evolve by Brownian dynamics into the specified multi-chain system by 'switching on' the bonding interaction, initially having a very long range (up to half the simulation cell size), in the absence of hydrophobic or electrostatic interactions. During this stage it is as if the adjacent segments in the chains are connected by long imaginary penetrable thin strings. Under the influence of this long-range hypothetical bonding potential, the 'strings' become gradually shorter until the separation between bonded segments approaches that of the equilibrium bond length (r_0). Once all the 81 chains had been generated, the hydrophobic and electrostatic forces were switched on, and the simulation proper was begun.

The time required for a simulated system to reach equilibrium varies according to the polymer volume fraction and the interaction parameters. Typically, the equilibration time is around 10^5 timesteps. The hard-sphere core potential was allowed for in the Brownian dynamics scheme by rejecting particle displacements that led to unphysical overlap between segments ($r < \sigma$) on the same or different chains. At constant particle volume fraction ϕ, the main factor affecting the rejection rate is the hydrophobic interaction energy ϵ_h. So, for example, at $\phi = 0.2$, the proportions of rejected (over-lapping) configurations are 12%, 25% and 40% for $\epsilon_h = 0.005$, 0.05 and 0.5, respectively.

4. Results and discussion

We first consider the effects of the values of the hydrophobic and electrostatic interaction parameters, ϵ_h and ϵ_e, on the structures of simulated systems at moderate volume fraction $\phi = 0.2$. Fig. 3 shows three-dimensional images for a set of configurations with constant $\epsilon_e = 1.0$ and different ϵ_h values of 0.005, 0.05, 0.5 and 5. We can see that the effect of increasing ϵ_h is to cause an increase in the heterogeneity of the segment density, with the co-polymer aggregates becoming more compact and less well incorporated into a gel-like network structure. This is confirmed in Table 2 by the value of the mean local segment co-ordination number which decreases from just above 2 (slightly branched chains) for very small ϵ_h (0.005, 0.05) to ca. 4 (clusters) for moderately large ϵ_h (0.5) [and to >10 for very large ϵ_h (5)].

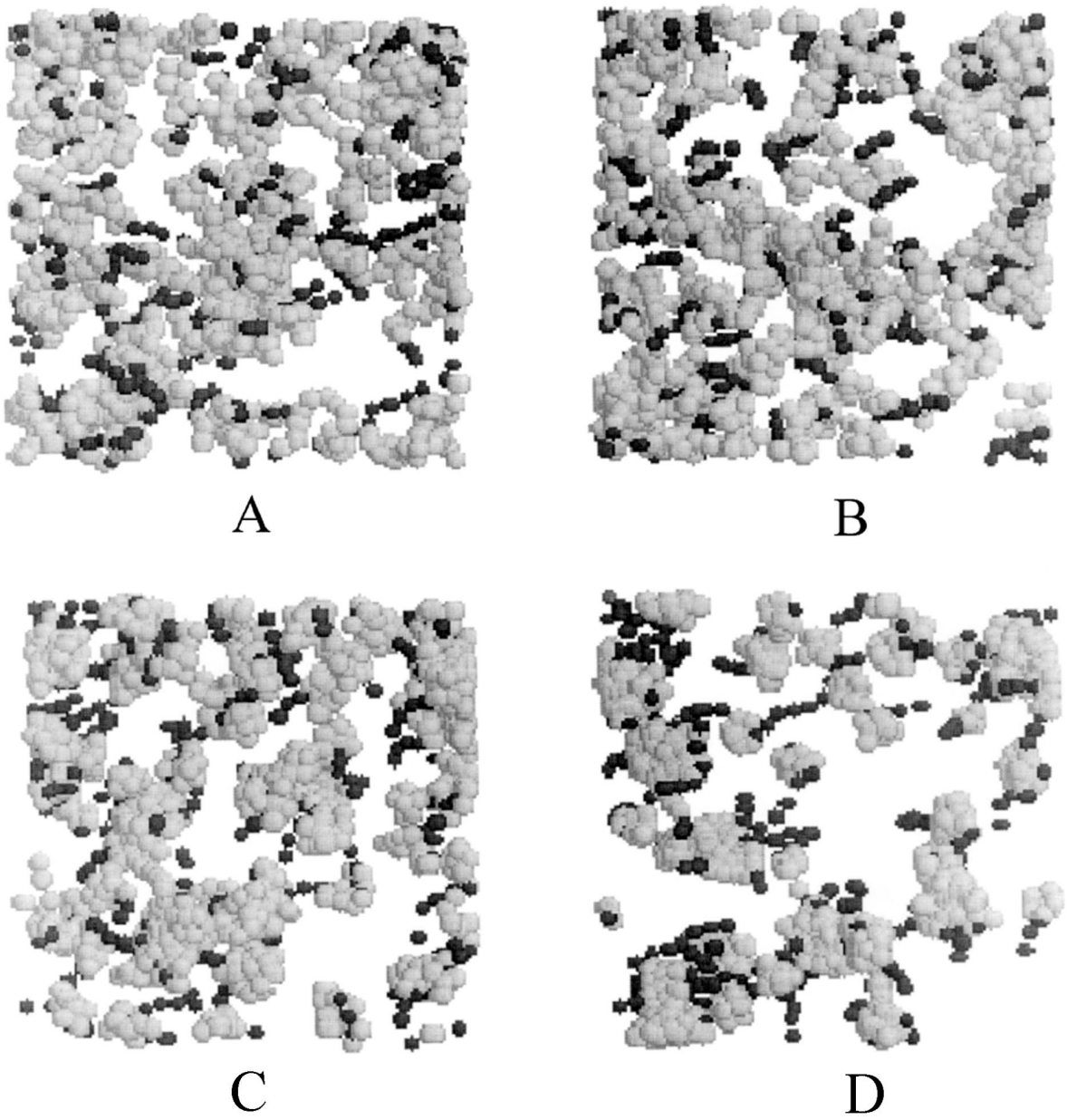


Fig. 3. Snapshots of equilibrated simulated systems (one unit cell) at volume fraction $\phi = 0.2$. Other parameter values are as in Table 1 except for the hydrophobic interaction energy ϵ_h which has values of: (a) 0.005, (b) 0.05, (c) 0.5 and (d) 5.

For each simulated configuration, we define the size of an aggregate as the total number of chains that are connected together topologically by the presence of at least one hydrophobic segment located on one chain lying within the interaction range of another hydrophobic segment on another chain. Of particular interest is the maximum aggregate size, S_{max}, since an indicator of gel-like network character is that most of the particles are incorporated into a small number of large aggregates. Fig. 4 shows the fluctuating average maximum aggregate size for systems with $\epsilon_h = 0.005$, 0.05, 0.5. (Data for the strongly interacting system with $\epsilon_h = 5.0$ are not shown because this does not reach equilibrium over the normal simulation timescale.) We see that the maximum aggregate size becomes reduced from $S_{max} = 23 \pm 4$ at $\epsilon_h = 0.005$ to $S_{max} = 9 \pm 1$ at $\epsilon_h = 0.5$. Weak gel-like character, generated through hydrophobically driven chain–chain associations, is favoured in structural terms by a relatively small finite value of the hydrophobic segment interaction energy.

In the set of configurations illustrated in Fig. 3, the hydrophilic segments play a role in maintaining the solubility (dispersion) of the co-polymer chains through repulsive electrostatic interactions. This is illustrated by the set of three configurations in Fig. 5 with constant and different ϵ_e values of 0, 1.0 and 4.0. Let us note first that Fig. 5(b) ($\epsilon_h = 0.05$, $\epsilon_e = 1.0$) is identical to Fig. 3(b). Switching off the electrostatic interaction (Fig. 5(a)) leads to a more phase-separated structure with a larger maximum aggregate

Table 2
Average segment co-ordination number of simulated systems as a function of (a) hydrophobic interaction energy (ϵ_h), (b) electrostatic interaction energy (ϵ_e) and (c) volume fraction (ϕ). The co-ordination number is defined as the number of segments with centres lying within 1.5 σ of a given segment. Other non-specified parameters take the values given in Table 1

Constant parameters	Variable parameter	Average co-ordination number
(a) $\epsilon_e = 1.0$, $\phi = 0.2$	$\epsilon_h = 0.005$	2.12
	$\epsilon_h = 0.05$	2.30
	$\epsilon_h = 0.5$	4.1
	$\epsilon_h = 5$	10.7
(b) $\epsilon_h = 0.05$, $\phi = 0.2$	$\epsilon_e = 0.5$	2.42
	$\epsilon_e = 1.0$	2.30
	$\epsilon_e = 4.0$	2.14
(c) $\epsilon_h = 0.05$, $\epsilon_e = 1.0$	$\phi = 0.1$	2.14
	$\phi = 0.2$	2.30
	$\phi = 0.3$	2.42

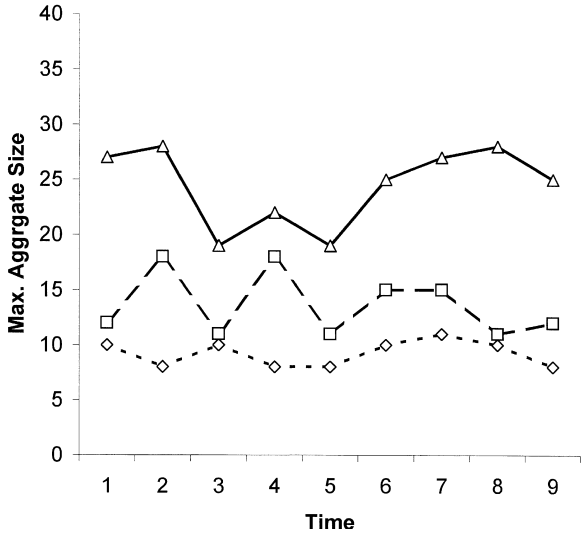


Fig. 4. Average maximum aggregate size with time for simulated systems pictured in Fig. 3: △, $\epsilon_h = 0.005$; □, $\epsilon_h = 0.05$; ◇, $\epsilon_h = 0.5$. One unit of time is 10^4 iterations.

size (Fig. 6) and an increased segment co-ordination number (Table 2). This is due to the passive role of the uncharged tail segments which become incorporated within a weakly phase-separating local network of predominantly hydrophobic chains. Conversely, when the electrostatic interaction energy is increased to $\epsilon_e = 4.0$, the structure becomes dominated by charge repulsion effects. The hydrophilic segments are completely driven out of the hydrophobic clusters, to produce a more uniform overall segment density, a lower segment co-ordination number (Table 2) and a slightly smaller maximum aggregate size (Fig. 6). Variation in the parameter ϵ_e can be regarded as being tentatively related to effects of changes in pH and ionic strength in real experimental casein systems. The explicit consideration of such experimental variables will become more appropriate in refined extensions of the present model, which may perhaps involve 3 or 4 different kinds of segment types, as opposed to the just two types considered in this preliminary mesoscopic simulation study.

All the simulated structures described above refer to a constant volume fraction of $\phi = 0.2$. For the case of the system with the standard interaction parameter settings ($\epsilon_h = 0.05$, $\epsilon_e = 1.0$), Figs. 7 and 8 show the effect of changing the value of ϕ to 0.1 or 0.3. We can see that the visible degree of connectivity (Fig. 7) and the maximum aggregate size (Fig. 8) are strongly influenced by this volume fraction parameter. At the low volume fraction the average segment co-ordination number is approaching 2 and S_{max} is only 3 ± 1, whereas at $\phi = 0.3$ we have a considerably higher co-ordination number and $S_{max} = 33 \pm 8$.

Within the statistical uncertainties specified, and for hydrophobic interactions not too strong ($\epsilon_h < 1$), our numerical results were found to be independent of the initial random configuration of the N unbonded segments prior to 'switching on' the bonding interaction. For very strongly associating chains (e.g. $\epsilon_h = 5$), however, the initially

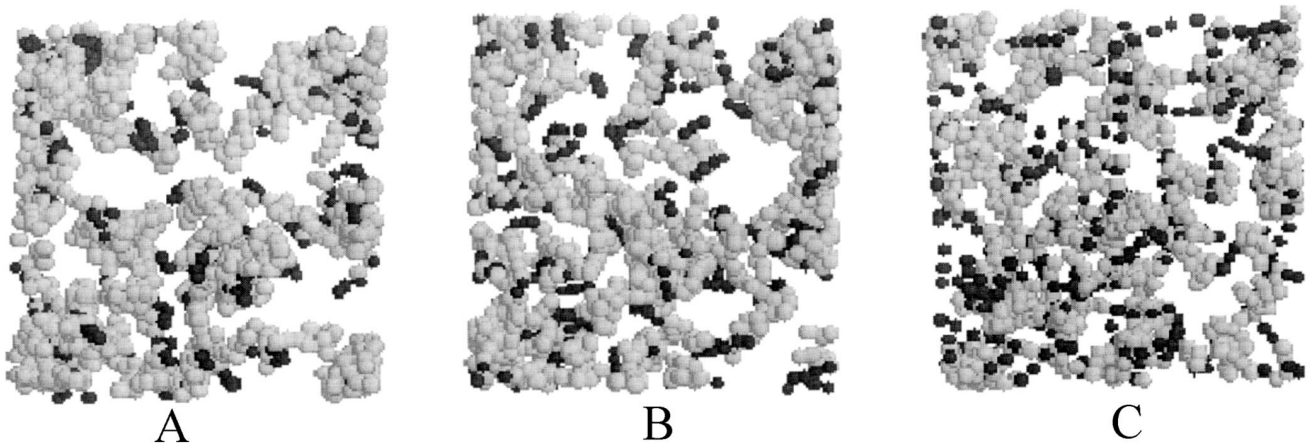


Fig. 5. Snapshots of simulated systems with $\phi = 0.2$ and other parameter values as in Table 1 except for the electrostatic interaction energy ϵ_e which has values of: (a) 0, (b) 1.0 and (c) 4.0.

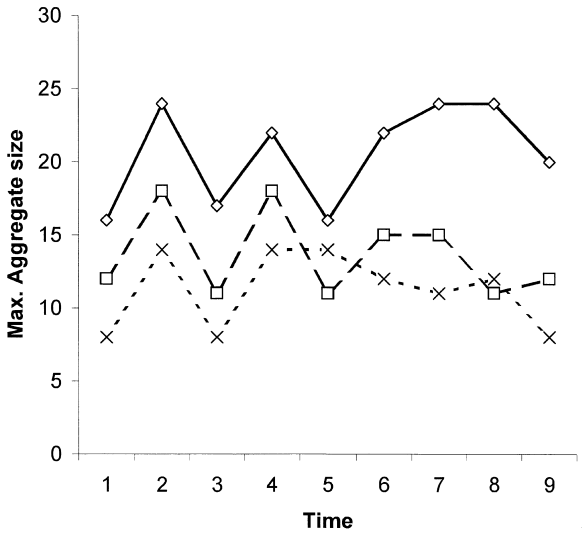


Fig. 6. Average maximum aggregate size with time for simulated systems pictured in Fig. 5: ◇, $\epsilon_e = 0$; □, $\epsilon_e = 1.0$; ×, $\epsilon_e = 4.0$. One unit of time is 10^4 iterations.

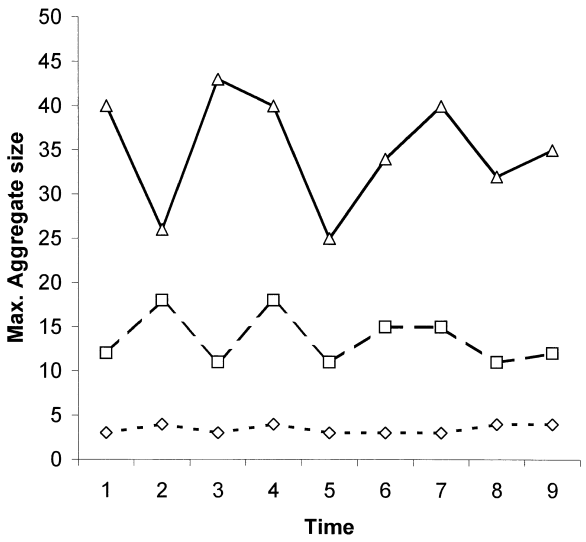


Fig. 8. Average maximum aggregate size with time for simulated systems pictured in Fig. 7: ◇, $\phi = 0.1$; □, $\phi = 0.2$; △, $\phi = 0.3$. One unit of time is 10^4 iterations.

induced aggregated structure gets 'locked in' to a metastable state with little local flexibility, and this state evolves only very slowly over the course of the simulation run time. It is known, of course, that slow ripening and ageing effects are important in real casein particle gel systems, with structural heterogeneities evolving on a spatial scale of 10^{-7}–10^{-5} m over time scales of up to minutes or even hours (Mellema, 2000). Unfortunately, the mesoscopic modelling of such time-dependent structural changes would appear to be beyond our currently accessible computer power.

We have, however, made a preliminary investigation of the local dynamics of the steady-state simulated systems by determining segment and chain diffusion coefficients. Fig. 9 shows the time-dependent mean-square displacement $\langle (r(t) - r(0))^2 \rangle$ for the segments at three different volume fractions in equilibrated systems with the standard interaction settings ($\epsilon_h = 0.05$, $\epsilon_e = 1.0$). The slopes of these lines give the mean segment diffusion coefficients D_S listed in Table 3. As expected, the segment mobility decreases with increasing volume fraction, the value at $\phi = 0.3$ being less than one half that at $\phi = 0.1$. Also shown in Table 3 are values of the chain diffusion coefficients D_C based on the slope of the mean-square displacement of the chain centre of mass. We see that D_C is much more concentration dependent than D_S. This can be explained in terms of a greater enhancement of chain–chain interactions than segment–segment interactions with increasing volume fraction.

5. Concluding remarks

The motivation for this mesoscopic approach is to provide a framework for simulating concentrated casein solutions and gels. The relative proportions of the two types of segments in the idealized co-polymer chain were chosen with the known primary structure of β-casein in

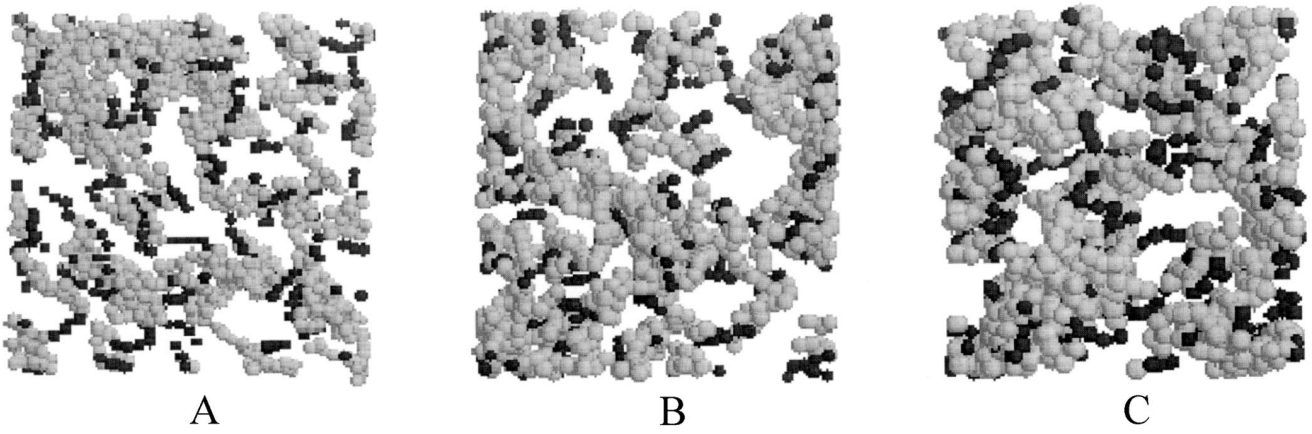


Fig. 7. Snapshots of simulated systems for different volume fractions with other parameter values as in Table 1: (a) $\phi = 0.1$, (b) $\phi = 0.2$ and (c) $\phi = 0.3$.

Table 3
Effect of volume fraction ϕ on the ensemble average values of the segment diffusion coefficient D_S and the chain diffusion coefficient D_C. Other parameters take the values given in Table 1

ϕ	D_S (10^{-6} cm^2 s^{-1})	D_C (10^{-6} cm^2 s^{-1})
0.1	1.32	1.11
0.2	1.07	0.79
0.3	0.56	0.26

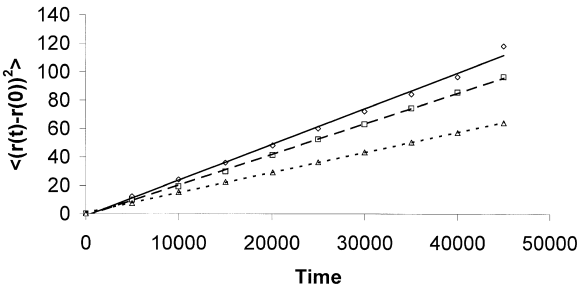


Fig. 9. Segment mean-square displacement $\langle (r(t) - r(0))^2 \rangle$ (in nm^2) for different volume fractions with other parameter values as in Table 1: ×, $\phi = 0.1$; □, $\phi = 0.2$; △, $\phi = 0.3$.

mind. However, through simple adjustment of the two available interaction parameters (ϵ_h and ϵ_e) in our computer experiments, we have not been able to reproduce the formation of the roughly spherical micelle-type structures that are consistent with published laboratory experiments on moderately dilute β-casein solutions (Schmidt, 1982; Leclerc & Calmettes, 1997). This could be because most of the experimental observations on β-casein micellization were carried out at volume fraction levels several orders of magnitude lower than those considered in our simulation. A more likely explanation, however, is that our assumed sub-division into 25% hydrophilic and 75% hydrophobic segments is not appropriate, because it implies an effective head-group size that may be too small (even for a high value of ϵ_e) to be properly conducive to the packing of the16-segment amphiphiles into conventional spherical micellar structures (Israelachvili, 1985). Moreover, it may be too much to expect that a molecule as complicated as a protein can be represented as a block co-polymer containing just two kinds of monomers (Shakhnovich, 1997).

Based on the preliminary results presented here, it is proposed that further modelling work should explore a more refined mesoscopic model of β-casein based on a palette of 4 ± 1 different kinds of segments, as successfully used in self-consistent-field modelling of β-casein adsorption (Leermakers et al., 1996) and in statistical modelling of protein folding (Wang & Wang, 2000). This same approach could then be used to compare β-casein with α_{s1}-casein (Dickinson, Horne, Pinfield, & Leermakers et al., 1997), and then eventually to simulate self-assembly in mixed solutions of different individual casein (to imitate sodium caseinate). Once these adjustments have been successfully made, there will be value in studying how raw parameters such as ϵ_h and ϵ_e can be related to variables in more refined interaction potentials that are explicitly sensitive to the main factors (pH, ionic strength, Ca^{2+} content) influencing the known experimental self-assembly behaviour of casein solutions and dispersions. For proper identification of gel-like character, there is clearly also a need to compute the small-deformation rheological properties as has been done previously for simple spherical particle gel systems (Whittle & Dickinson, 1997). Subject to continued modifications and refinements, this approach provides a framework for systematically understanding the effects of protein content and solution conditions in concentrated self-assembled casein systems.

Acknowledgements

We thank a referee for constructive comments. E. D. acknowledges financial support for this research from the Biotechnology and Biological Sciences Research Council.

References

Allen, M. P., & Tildesley, D. J. (1989). *The computer simulation of liquids*, Oxford: Oxford University Press.

Anderson, R. E., Pande, V. S., & Radke, C. J. (2000). Dynamic lattice Monte Carlo simulation of a model protein at an oil/water interface. *Journal of Chemical Physics*, *112*, 9167–9185.

Berry, G. P., & Creamer, L. K. (1975). The association of bovine β-casein. *Biochemistry*, *14*, 3542–3545.

Bijsterbosch, B. H., Bos, M. T. A., Dickinson, E., van Opheusden, J. H. J., & Walstra, P. (1995). Brownian dynamics simulation of particle gel formation: from argon to yoghurt. *Faraday Discussions*, *101*, 51–64.

Boyd, R. H., & Phillips, P. J. (1993). *The science of polymer molecules*, Cambridge: Cambridge University Press.

Brooks, B. R., Bruccoleri, R. E., Olafson, B. D., States, D. J., Swaminathan, S., & Karplus, M. (1983). CHARMM—A program for macromolecular energy, minimization and dynamics calculations. *Journal of Computational Chemistry*, *4*, 187–217.

Chu, B., Zhou, Z., Wu, G., & Farrell Jr., H. M. (1995). Laser light scattering of model casein solutions: effects of high temperature. *Journal of Colloid and Interface Science*, *170*, 102–112.

Creamer, L. K., & Berry, G. P. (1975). A study of the properties of dissociated bovine casein micelles. *Journal of Dairy Research*, *42*, 169–183.

Dalgleish, D. G. (1996). Conformations and structures of milk proteins adsorbed to oil–water interfaces. *Food Research International*, *29*, 541–547.

Dickinson, E. (1997). Aggregation processes, particle interactions, and colloidal structure. In E. Dickinson & B. Bergenståhl, *Food colloids: proteins, lipids and polysaccharides* (pp. 107–126). Cambridge: Royal Society of Chemistry.

Dickinson, E. (1998). Proteins at interfaces and in emulsions: stability, rheology and interactions. *Journal of the Chemical Society, Faraday Transactions*, *94*, 1657–1669.

Dickinson, E. (1999). Caseins in emulsions: interfacial properties and interactions. *International Dairy Journal*, *9*, 305–312.

Dickinson, E., Horne, D. S., Pinfield, V. J., & Leermakers, F. A. M. (1997). Self-consistent-field modelling of casein adsorption: comparison of results for α_{S1}-casein and β-casein. *Journal of the Chemical Society, Faraday Transactions*, *93*, 425–432.

Farrer, D., & Lips, A. (1999). On the self-assembly of sodium caseinate. *International Dairy Journal*, *9*, 281–286.

Ganazzoli, F. (2000). Globular state of random polymers with arbitrary amphiphilicity. *Journal of Chemical Physics*, *112*, 1547–1553.

Horne, D. S. (1998). Casein interactions: casting light on the black boxes, the structure in dairy products. *International Dairy Journal*, *8*, 171–177.

Horne, D. S., & Leaver, J. (1995). Milk proteins on surfaces. *Food Hydrocolloids*, *9*, 91–95.

Israelachvili, J. N. (1985). *Intermolecular and surface forces*, London: Academic Press.

Leclerc, E., & Calmettes, P. (1997). Interactions in micellar solutions of β-casein. *Physical Review Letters*, *78*, 150–153.

Leermakers, F. A. M., Atkinson, P. J., Dickinson, E., & Horne, D. S. (1996). Self-consistent-field modelling of adsorbed β-casein: effects of pH and ionic strength on surface coverage and density profile. *Journal of Colloid and Interface Science*, *178*, 681–693.

Lodge, J. F. M., & Heyes, D. M. (1999). Transient colloidal gels by Brownian dynamics computer simulation. *Physical Chemistry Chemical Physics*, *1*, 2119–2130.

Lucey, J. A., Srinivasan, M., Singh, H., & Munro, P. A. (2000). Characterization of commercial and experimental sodium caseinates by multi-angle laser light scattering and size-exclusion chromatography. *Journal of Agricultural and Food Chemistry*, *48*, 1610–1616.

Mellema, M. (2000). *Scaling relations between structure and rheology of ageing casein particle gels. Ph.D. thesis*, Netherlands: Wageningen University.

Mellema, M., van Opheusden, J. H. J., & van Vliet, T. (1999). Relating colloidal particle interactions to gel structure using Brownian dynamics simulations and the Fuchs stability ratio. *Journal of Chemical Physics*, *111*, 6129–6135.

Morse, P. M. (1929). Diatomic molecules according to the wave mechanics. II. Vibrational levels. *Physical Review*, *34*, 57–64.

Schmidt, D. G. (1982). Association of caseins and casein micelle structure. In P. F. Fox, *Developments in dairy chemistry* (pp. 61–86). London: Applied Science.

Schmidt, D. G., & Payens, T. A. J. (1972). The evaluation of positive and negative contributions to the second virial coefficient of some milk proteins. *Journal of Colloid and Interface Science*, *39*, 655–662.

Shakhnovich, E. I. (1997). Theoretical studies of protein-folding thermodynamics and kinetics. *Current Opinion in Structural Biology*, *7*, 29–40.

Toma, L., & Toma, S. (2000). A lattice study of multimolecular ensembles of protein models. Effect of sequence on the final state: globules, aggregates, dimers, fibrillae. *Biomacromolecules*, *1*, 232–238.

Vreeman, H. J., Brinkhuis, J. A., & van der Spek, C. A. (1981). Some association properties of bovine SH-κ-casein. *Biophysical Chemistry*, *14*, 185–193.

Wang, J., & Wang, W. (2000). Modelling study on the validity of a possibly simplified representation of proteins. *Physical Review E*, *61*, 6981–6986.

Whittle, M., & Dickinson, E. (1997). Brownian dynamics simulation of gelation in soft sphere systems with irreversible bond formation. *Molecular Physics*, *90*, 739–757.